Science of the Total Environment 625 (2018) 647–656

Contents lists available at ScienceDirect

Science of the Total Environment

journal homepage: www.elsevier.com/locate/scitotenv

Landscape evolution and agricultural land salinization in coastal area: A conceptual model

Aplena Elen Bless [a,b], François Colin [a], Armand Crabit [a], Nicolas Devaux [a], Olivier Philippon [a], Stéphane Follain [a,*]

[a] LISAH, Montpellier SupAgro, INRA, IRD, Univ Montpellier, Montpellier, France
[b] Soil Science Department-Agricultural Faculty, Papua University, Manokwari, Papua, Indonesia

HIGHLIGHTS

- We investigated soil and water salinity in an agricultural coastal landscape.
- We drove a time analysis of climate, river and land system since 1962.
- We proposed a conceptual model of water fluxes for salt affected lands.
- Landscape evolutions were responsible for system equilibrium disruption.
- Natural and human induced changes favored salt accumulation in soil root zone.

GRAPHICAL ABSTRACT

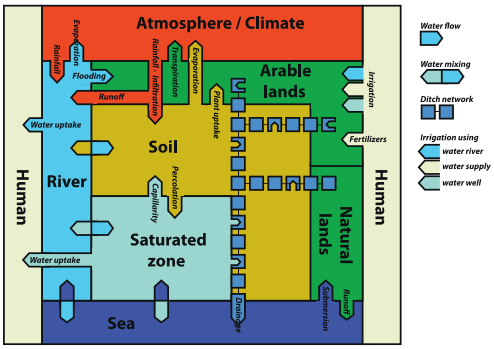

ARTICLE INFO

Article history:
Received 31 August 2017
Received in revised form 7 December 2017
Accepted 7 December 2017
Available online xxxx

Editor: Jay Gan

Keywords:
Coastal landscape
Conceptual model
Salinization
Vineyard

ABSTRACT

Soil salinization is a major threat to agricultural lands. Among salt-affected lands, coastal areas could be considered as highly complex systems, where salinization degradation due to anthropogenic pressure and climate-induced changes could significantly alter system functioning. For such complex systems, conceptual models can be used as evaluation tools in a preliminary step to identify the main evolutionary processes responsible for soil and water salinization. This study aimed to propose a conceptual model for water fluxes in a coastal area affected by salinity, which can help to identify the relationships between agricultural landscape evolution and actual salinity. First, we conducted field investigations from 2012 to 2016, mainly based on both soil ($EC_{1/5}$) and water (EC_w) electrical conductivity survey. This allowed us to characterize spatial structures for $EC_{1/5}$ and EC_w and to identify the river as a preponderant factor in land salinization. Subsequently, we proposed and used a conceptual model for water fluxes and conducted a time analysis (1962–2012) for three of its main constitutive elements, namely climate, river, and land systems. When integrated within the conceptual model framework, it appeared that the evolution of all constitutive elements since 1962 was responsible for the disruption of system equilibrium, favoring overall salt accumulation in the soil root zone.

1. Introduction

Land resources are being irreversibly lost and degraded due to pressure generated by human populations and activities and by changes in climate and land use (EEA, 2000). For agricultural lands, anthropogenic changes are induced by farmers at both field unit and farm scale or by

* Corresponding author.
E-mail address: follain@supagro.fr (S. Follain).

https://doi.org/10.1016/j.scitotenv.2017.12.083
0048-9697/

policymakers from farming to administrative divisions (Verburg et al., 2002; Rounsevell et al., 2005; Claessens et al., 2009). Climate-related changes are induced by climate factors as predicted by projections of future climate change (IPCC Core Writing Team, 2014).

Within this context of land degradation, soil salinization is a major threat. According to FAO in 2000, around 830 Mha of land worldwide contains salt-affected soil (SAS) (Martinez-Beltran and Manzur, 2005). SAS can be found on all continents apart from Antarctica and occurs in >100 countries worldwide (Szabolcs, 1985; Rengasamy, 2006), with the most prominent areas being arid and semiarid climatic zones. In Europe, soil salinity affects about 3.8 Mha of land (Tóth et al., 2008; Rhoades et al., 1999; JRC, 2012) and is particularly problematic in the coastal areas of southern Europe (Daliakopoulos et al., 2016). Salinization is an increase in the concentration of water-soluble salts in water and soils. Soluble salts could be of environmental origin (geological, climatic, topographic, and hydrological) or result from inefficient or inappropriate human activities (Shrestha, 2006; Szabolcs, 1992; Daliakopoulos et al., 2016). Whatever the origin, salinity threatens the sustainability of agriculture by affecting crop production through decreased yields and plant death (Feinerman et al., 1982; Maas and Hoffman, 1977; Li et al., 2012), according to processes summarized by Rengasamy (2010).

In order to preserve land resources and crop production potential, a possible solution to salinization is the promotion of sustainable land management practices that sustainably reduce salinity. To this end, modeling is an appropriate method for simulating the evolution of soil salinity according to different land management scenarios. Daliakopoulos et al. (2016) and Coletti et al. (2017) have listed models for studying the evolution of salinity in agricultural environments. However, the use of these models presumes the ability of users to produce quantitative data and to have hypotheses on system functioning and complexity. A preliminary step prior to this numerical work could be to use a conceptual model as an evaluation tool, allowing the reduction of complexity (Margoluis et al., 2009).

Estuaries are defined as areas where salt water from the ocean mixes with fresh water from land drainage (Potter et al., 2010; Whitfield and Elliot, 2011). For centuries, estuarine wetland ecosystems have been valuable to humans. Now, estuaries have become hotspots not only for agricultural land use but also for human settlements, tourism, and industries. Due to this anthropogenic pressure, estuaries are susceptible to land degradation and ecosystem disturbances. Indeed, estuaries represent highly complex situations, e.g., situations where social, political, economic, cultural, and environmental factors interact (Brechin et al., 2002; Hannah et al., 2002). In France, the Orb River estuary is an appropriate example of agricultural land where conceptual models could be helpful in identifying the main factors of land salinization.

Consequently, the objectives of this study were (i) to determine actual soil and water salinity in the Orb estuary, (ii) to determine the landscape evolution, and (iii) to build a conceptual model of water fluxes in a coastal area affected by salinization in order to identify the relationship between landscape evolution and actual salinity.

2. Materials and methods

2.1. Study area

The study area is located in the Orb River delta connected to the Mediterranean Sea (Fig. 1). Research was conducted in the Sérignan municipality (43°28′N; 3°31′E) where the main human activities are viticulture and tourism. Over the last decade, there has been a yield reduction in wine production and winegrowers generally assumed that soil salinization is the trigger. Interviews between the local authority and the local winegrowers' association (Cave Coopérative Les Vignerons de Sérignan) in 2016 estimated that around 43% of Sérignan vineyard soil surfaces has been affected by salinization over the last decade.

From a geomorphic perspective, Sérignan is located in a sedimentary basin of alluvial origin (Orb River) connected to the Mediterranean

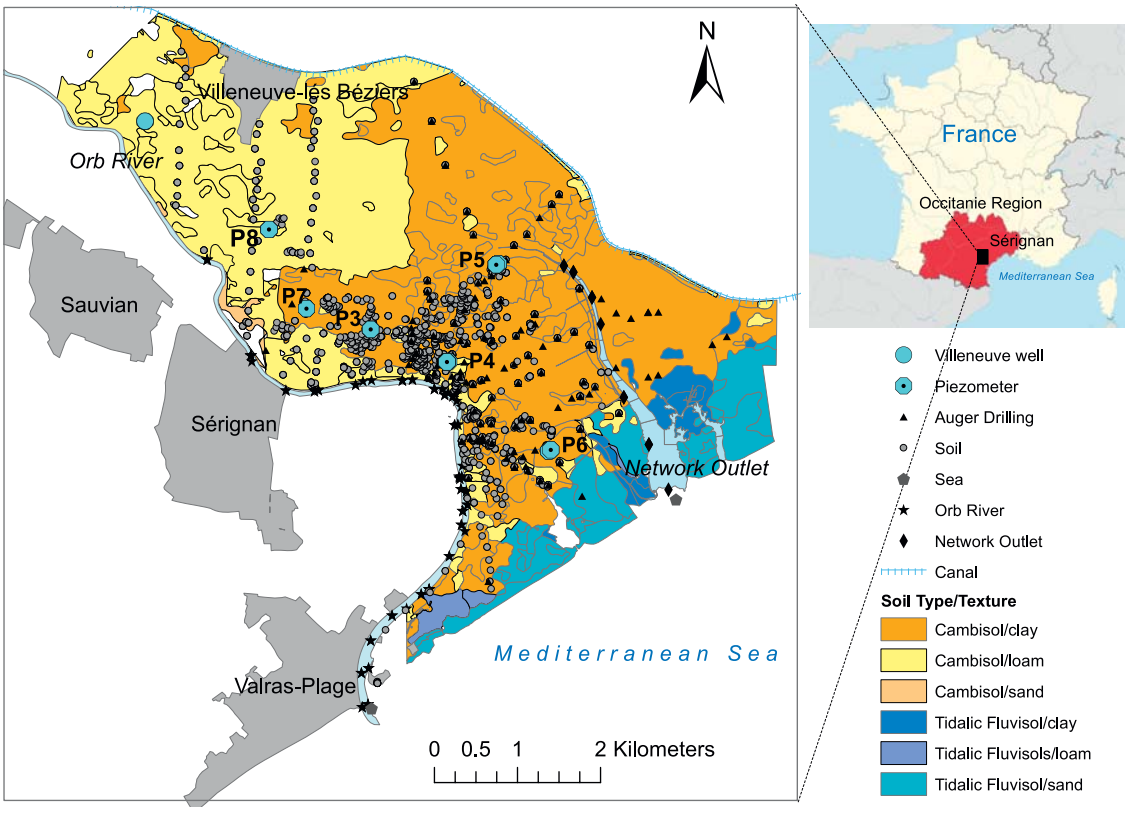

Fig. 1. Map of soil type and texture in the study area (Sérignan, France) and sampling locations for soil and water (piezometer, auger drilling, Orb River, network outlet, and sea) sampled from year 2012 to 2016.

coastline. In the central part, the sedimentary basin is topographically flat and consists of recent alluvium sediments. High elevations in relation to old alluvium and colluvium sediments characterize basin borders. Near the seashore, alluvial deposits are substituted by fluvial-lacustrine deposits and dune formation. Elevation ranges from 3 to 6 m.a.s.l. and saturated soil depth is approximately 2–4 m from the soil surface. The Sérignan aquifer system can be categorized as a "thick multilayered coastal aquifer system", according to the categorization by Custodio (2002). Between the soil surface and −100 m, the system is composed of several small unconfined aquifers. Within this multilayered system, our study focused on the first superficial unconfined aquifer developed in Quaternary and Pliocene materials within the first 10 m. The associated water table that we worked on is the water-saturated zone of soil cover connected with the Orb River alluvial aquifer. The first confined aquifer is located between −100 and −140 m. This confined aquifer (Pliocene–Piazencian) is composed of sandy materials and is a freshwater source for human use.

In this estuarine context, soil spatial distribution is clearly linked to material of alluvial and tidal origin (Barriere et al., 1973; Bless et al., 2017). In the northern part of study area, dominated by alluvial material, the main soil type is Cambisols (WRB, 2015), with a soil texture dominated by the silt fraction and a texture gradient towards more loamy or clayey texture with increasing soil depth (Fig. 1). Next to the seashore, the soil type is Tidalic Fluvisols (WRB, 2015), constituted from both lacustrine and marine sediments. Present-day agricultural production is mainly located on Cambisols characterized by pH values ranging from 8.0 to 8.5, total carbonate content ranging from 410 to 639 ppm (Calcaric Cambisols), and specifically the high soil organic carbon content (~22.5 g kg^{-1}) (Cave cooperative de viticulteurs de Sérignan, 2016) when compared to mean soil organic carbon (13.2 g kg^{-1}) of the vineyard at the Herault Department (Salome et al., 2014). Whatever the soil type, the soil profile horizonation is influenced by soil tillage with the A-horizon in the first 40 cm (deep tillage), the deep A-horizon at depths between 40 and 60–70 cm, and mineral horizons (B-type) at depths of over 60–70 cm (Bless et al., 2017).

The climate is of Csa type (Köppen-Geiger classification). According to data records from the Béziers-Vias meteorological station (43°19′N; 3°21′E) the wet season has been from September to April with maximum precipitation in November, and the dry season is from May to August, with maximum monthly reference evapotranspiration (ET0) in August. The Orb River is 135.4 km long and flows into Mediterranean Sea in Sérignan–Valras-Plage. The Orb River catchment area at the sea outlet is 1585 km^2 with altitudes ranging between 1126 and 0 m.a.s.l. Along the river, a dam was built in 1962 in the upstream part of the watershed and several pumping stations ensure irrigation and drinking water supply.

Main agricultural uses are viticulture, crops (durum wheat, peas and barley) and pasture. Agriculture is dominated by viticulture since the end of the 19th century. Agricultural practices had substantially changed with time, with transition from horses to engines for soil tillage and chemical weeding in the second part of twentieth century. The traditional salinity management in the coastal area was field submersion and drainage of percolation water through ditch network. Initially, Orb River was the only fresh water source for submersion through direct pumping or natural flooding. Later, additional source of fresh water was started in the 1960s using irrigation water pipes.

2.2. Data collection

2.2.1. Soil and water salinity

To estimate soil and water salinity, we used the relationship by Richards (1974) that relies on the electrical conductivity of saturated paste extracts and total dissolved salts. In order to perform a high number of measurements, electrical conductivity with temperature corrections was measured using a Consort K912 probe (Consort bvba, Belgium) with (i) direct measurement for water (EC_w) and (ii) a 1:5 ratio of soil to deionized water for soil ($EC_{1/5}$). Fig. 1 shows the spatial distribution of soil and water sampling locations. Soil samples (N = 1737) were collected for different soil depths (0.20, 0.50, 0.80, 1.10, and 1.20 m) using a soil auger in two contrasting months: at the end of September (dry season) and the end of March (wet season) from 2012 to 2016. Each auger boring for the soil sampling survey was conducted according to FAO rules for soil description (Jahn et al., 2006). All soil samples were air-dried and measured for $EC_{1/5}$ following the protocol of the United States Salinity Laboratory (Rhoades et al., 1999). Saturated soil depth was determined by drilling 102 holes using the prospecting kit for geological surveys by Eijkelkamp (The Netherlands). For each hole, we waited for water level equilibrium before noting saturated soil depth, sampling water, and measuring EC_w. Additional EC_w measurements were taken in the agricultural fields, Orb River, ditch network, network outlet, and sea.

Additional samples were collected for the determination of classical chemical parameters. For soil samples, pedological trenches were dug in order to describe the main soil morphological traits and properly sample soil volume per soil horizon type. For water samples, six piezometers (2.0–4.0 m in depth) distributed across the study area were built and sampled in 2016 during both the wet and dry seasons. In order to compare our data to local reference values, we collected data of fresh groundwater from (i) the French National Data Base on groundwater and (ii) data from "Villeneuve" and "Raysac." Piezometers. The sodium adsorption ratio (SAR) was calculated from the ratio of Na^+ and the square roots of total Ca^{2+} and Mg^{2+} contents divided by two (Richard, 1954).

We analyzed the data statistically via SPSS 22 software. As the data were not normally distributed according to the Kolmogorov–Smirnov test for normality, we did the nonparametric Kruskal–Wallis test to determine the overall significant difference, followed by Wilcoxon test to identify particular classes that were significantly different.

2.2.2. Landscape evolution data

Annual and monthly mean temperature and rainfall time-series were constructed from the extraction of the CRU TS v. 3.24.01 gridded dataset of the Climatic Research Unit (School of Environmental Sciences, University of East Anglia) (Harris et al., 2014). The extracted half-degree gridbox (43°15′N; 3°15′E) is centered near Sérignan and the time-series concerned the period of 1960–2015. We calculated monthly ET0 using the formula of Thornthwaite (1948). Annual ET0 was calculated by summing the monthly values. The annual climatic water deficit was calculated as the difference between annual ET0 and the annual rainfall amount.

The Orb River discharges were measured from 1965 to 2015 at Béziers-Tabarka hydrological station (43°22′N; 3°10′E) by DREAL-Languedoc Roussillon. The station is located downstream of the catchment, at a distance of 8 km from the coastline. From the time-series, we calculated the annual mean discharges (AMD) and the lowest monthly discharges per hydrological year (LMD). Climatic and discharge trends were calculated using the 10-year moving average applied to the annual data with R-software.

An important issue was to analyze landscape structure and land use evolution. The first action was to select two different years using an approach that combines local farmers' perceptions of landscape changes and factual descriptions of landscape design (e.g., aerial photographs from the French National Geographic Institute from 1942 to present). This procedure allowed us to select aerial photographs from 1962 and 2012. 1962 is the year prior to governmental coastal land dimensioning programs. 2012 is the year with the highest quality aerial photography and having the same landscape structure as that of 2007–2010 (the period when yield decreases started). The second action was to drive visual recognition and manual digitalization of land uses and landscape structures using ArcGIS software. To validate past land uses and land cover allocations, we conducted additional interviews with aged farmers.

3. Results

3.1. Water and soil salinity

Water geochemistry and electrical conductivity results are presented in Table 1. Measured EC_w values from piezometers ranged from 1.43 to 5.74 dS m^{-1} and calculated SAR values ranged from 1.19 to 24.15. Two piezometers, P6 and P8, seemed less affected by salinity from seawater as indicated by their low Na^+ and Cl^- contents. P8 was located in the northern part of the study area, where the distance from the sea is the farthest (5.6 km), and exhibited ionic composition close to that of the "Villeneuve" considered as freshwater reference. The location of P8 contrasted that of P6, which was the nearest to the sea (1.2 km). Piezometers P3, P4, P5, and P7 indicated higher salinity levels: EC_w values ranged from 2.97 to 5.74 dS m^{-1} and SAR values ranged from 5.34 to 24.15. P4 and P7 had the highest Na^+ contents and the highest EC_w values, and the EC_w value of P7 (5.74 dS m^{-1}) indicated that the contents of all cations and anions were high.

Results for EC_w measured at different water sources in March and September are presented in Table 1. EC_w values ranged from 0.15 to 42.60 dS m^{-1} (excluding seawater). Ranking of mean or median values for EC_w provided the following order from high to low conductivity values: seawater > network outlet > ditch network > river > saturated zone. When comparing all standard deviation values, we noticed that the river was the most variable water source (standard deviation = 13.81 dS m^{-1}), followed by the ditch network (10.36 dS m^{-1}) and saturated zone measured during auger drilling (9.08 dS m^{-1}), whereas saturated zones measured by the piezometers had the lowest standard deviation value of around 3.00 dS m^{-1}. The saturated zone from auger drilling had the highest maximum value of 42.60 dS m^{-1}. Categorization of piezometer values in relation to time allowed analysis of the potential seasonal effect. In our measurements, descriptive statistics did not show any significant differences between the two time-series (p-value > 0.05).

In order to investigate the spatial distribution of electrical conductivity, all measured values for both water (from auger drilling) and soil were categorized according to the geographical distance (km) to the river (Fig. 2A1–B1) and sea (Fig. 2A2–B2). EC_w values categorized according to distance to the river showed a gradual decrease of median values for increasing distance (Fig. 2A1), from 5.18 dS m^{-1} in the vicinity of the river to 1.55 dS m^{-1} for the farthest distance. This trend in median values differed from that observed for variability as informed by inter-quartile values (3rd–1st quartile) and numerical values (maximum–minimum): the 1.0–1.5 km class was associated with higher variability, the 1.5–2.0 km class was associated with higher numerical extend and the >2 km class presents the lowest value regardless of the statistical parameter. For this categorization (EC_w ~ Orb), statistical tests showed that only extreme distance classes were significantly different (p-value < 0.05). The same representation of EC_w according to distance to sea (Fig. 2A2) offered a different spatial structure: a decrease in median EC_w inter-quartile and numerical values up to 1.5 km, then highest maximum and median values for intermediate classes of distance from 1.5 to 2.5 km, and a net decrease of median and inter-quartile values for distances of >2.5 km. The distribution of electrical conductivity values for soils (Fig. 2B1–B2) did not differ much from that of water, except for the numerical extends of values. Fig. 2B1 presents $EC_{1/5}$ value distributions of significantly different distance classes, namely 0.0–0.5 km and up to 2 km. Once again, the spatial structure of values was less marked when categorized according to distance to coast (Fig. 2B2), and significant differences are noticeable for the 1.5–2.0 and >3.5 km classes.

3.2. Landscape evolution

Fig. 3 presents landscape transitions from 1962 to 2012. Over 50 years, there were substantial changes in both land use and landscape design. From 1962 to 2012, the total number of arable field units decreased significantly, from 1674 to 679 fields, and the associated mean area for vineyards almost doubled, from 0.85 to 1.50 ha. During the same period, the mean size of crop and pasture fields increased by over three times. The total area of arable and natural land decreased by about 3 and 29%, respectively. This decrease was contemporaneous with an increase of four times in artificial buildings, mostly located near the coastline. Currently, 21% of vineyard land is new (i.e., where there were no vineyards in 1962) and located in the upper and central parts of the study area, whereas 36% of past vineyard land has now been converted to other land uses close to the river and the ditch network outlet. Additional results from interviews were related to the traditional landscape design associated with field unit borders, but that could not be recognized on 1962 aerial photographs. Old-field units were systematically bounded by ditch structures, creating a global ditch network for which the ditch network outlet was the outlet connection to the sea. The filling of old ditches using power shovels created a drastic increase in field area from 1962 to 2012.

The regional annual means of rainfall, temperature, and ET0 are shown in Fig. 4. The annual rainfall means ranged from 416 to 1015 mm with an interannual mean of 655 mm over the 1960–2015 period. Rainfall amount was the highest during the 1960s with annual

Table 1
Water geochemistry and water electrical conductivity (EC_w) at different water sources.

Water sources	Time	ECw (dS m^{-1})						Concentration (mmol/l)						ECw (dS m^{-1})	SAR
		N	Min	Max	Mean	Median	St. dev	Na^+	Ca^{2+}	Mg^{2+}	Cl^-	SO_4^{2-}	HCO_3^-		
EC_w saturated zone (piezometers)	Feb/Mar	71	0.53	12.83	4.93	4.13	3.06								
	Sep/Oct	50	0.58	12.10	4.82	4.02	3.35								
Name (water depth)															
P3 (2.2 m)								15.96	6.05	11.83	12.32	7.54	13.30	3.46	5.34
P4 (2.1 m)								40.48	1.70	3.92	28.81	1.79	13.39	4.72	24.15
P5 (1.5 m)								24.52	1.85	3.00	11.92	5.81	12.30	2.97	15.75
P6 (1.7 m)								2.83	5.90	5.42	2.60	5.15	6.61	1.43	1.19
P7 (3.1 m)								35.74	9.00	12.08	14.55	19.15	17.30	5.74	11.01
P8 (4.0 m)								7.30	10.95	11.17	6.89	8.71	10.10	2.95	2.20
Saturated zone (auger drilling)		101	0.15	42.60	8.00	4.20	9.08								
Saturated zone depth (m)		114	0.40	4.00		1.80									
Orb River		66	0.28	35.75	8.30	4.23	13.81								
Ditch network		79	2.23	38.17	15.22	14.87	10.36								
Network outlet		12	11.50	26.70	21.04	24.05	5.47								
E.Rayssac[a]								0.38	2.74	1.33	0.37	0.64	3.38	0.45	0.27
E.Villaneuf[a]								2.16	7.25	3.58	2.25	3.11	7.72	1.31	0.93
Sea[b]								469.57	20.55	106.67	546.61	56.50	1.80	54.75	58.88

[a] Freshwater.
[b] Salt water.

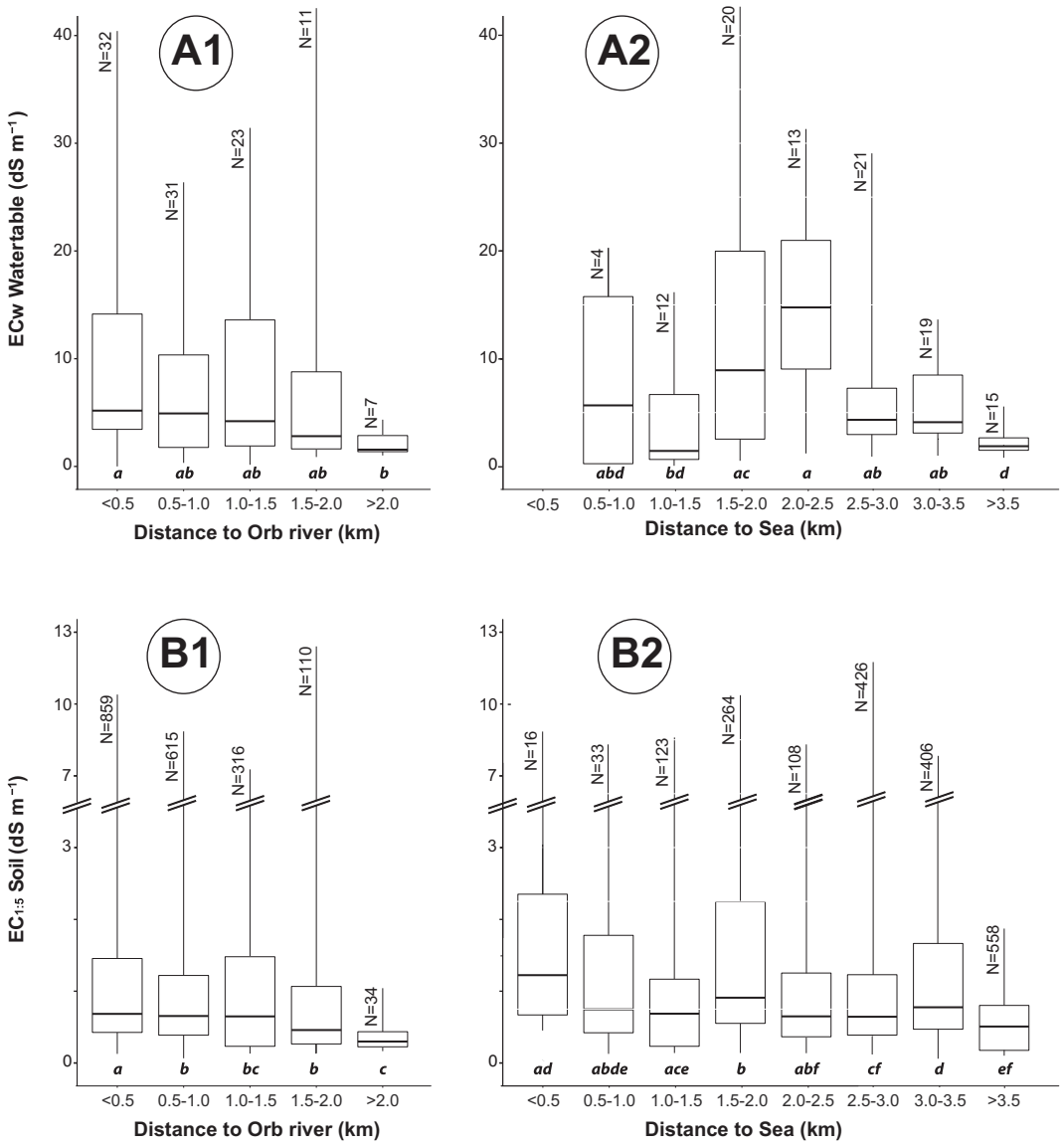

Fig. 2. Spatial distribution of electrical conductivity measured for both water (from auger drilling) and soil according to the geographical distance (km) to the river (A1–B1) and sea (A2–B2). Different letter means significant difference (p-value < 0.05).

rainfall of around 700 mm. The 1970s showed a transition to the dry years of the 1980s (630 mm per annum). The 1990s were rainy (675 mm per annum) before the driest decade between 2000 and 2010. Since 2010 there has been an increase to around 630 mm per annum. The mean annual temperature showed an overall increase from 1960 to 2015, with a higher rate at the end of the time-series. The mean annual temperature was <16 °C until 2004 and increased to over 18 °C within four last years. Despite a decrease in ET0 between 1960 and 1970, the trend showed a regular increase from 750 to 860 mm by 2005 and stabilizing thereafter. The annual climatic water deficit was highly variable between years with positive and negative values. The extreme years were 1996, when difference between rainfall and ET0 was −240 mm, and 2006 with a difference of 410 mm.

The AMD and LMD of the Orb River over the 1965–2015 period at the Béziers-Tabarka station are given in Fig. 5. The interannual mean discharge value over the period was 25.7 $m^3\ s^{-1}$, whereas AMD value ranges between 6.8 $m^3\ s^{-1}$ (2004–2005) and 69.0 $m^3\ s^{-1}$ (1995–1996). The AMD trend shows values around 28 $m^3\ s^{-1}$ along the time-series with two periods with a lower value of around 20 $m^3\ s^{-1}$ at the end of the 1980s and the beginning of the 2000s. However, the time-series of LMD was different: values were variable and decreased from the 1960s to the mid-1980s, when low flows were fewer and more stable. Three years exhibited particularly low LMD values, namely 1993–1994 (2.1 $m^3\ s^{-1}$), 1994–1995 (2.3 $m^3\ s^{-1}$), and 2005–2006 (2.0 $m^3\ s^{-1}$).

4. Discussion

4.1. Actual salinity

Land salinization management cannot be properly implemented without preliminary knowledge about spatial distribution and evolution of salinization (Michot et al., 2013). Our primary action was to quantify the spatial distribution of soil and water salinity. Considering the total area of agricultural land in our study area (170 km^2), we chose electrical conductivity (EC_w and $EC_{1/5}$) rather than classical extract paste measurements that exclude massive data collection. This choice was supported by other studies demonstrating that electrical conductivity is a proper variable for the estimation of salinity (from seawater origin) (Richards, 1974; Rhoades, 1997; Gkiougkis et al., 2015).

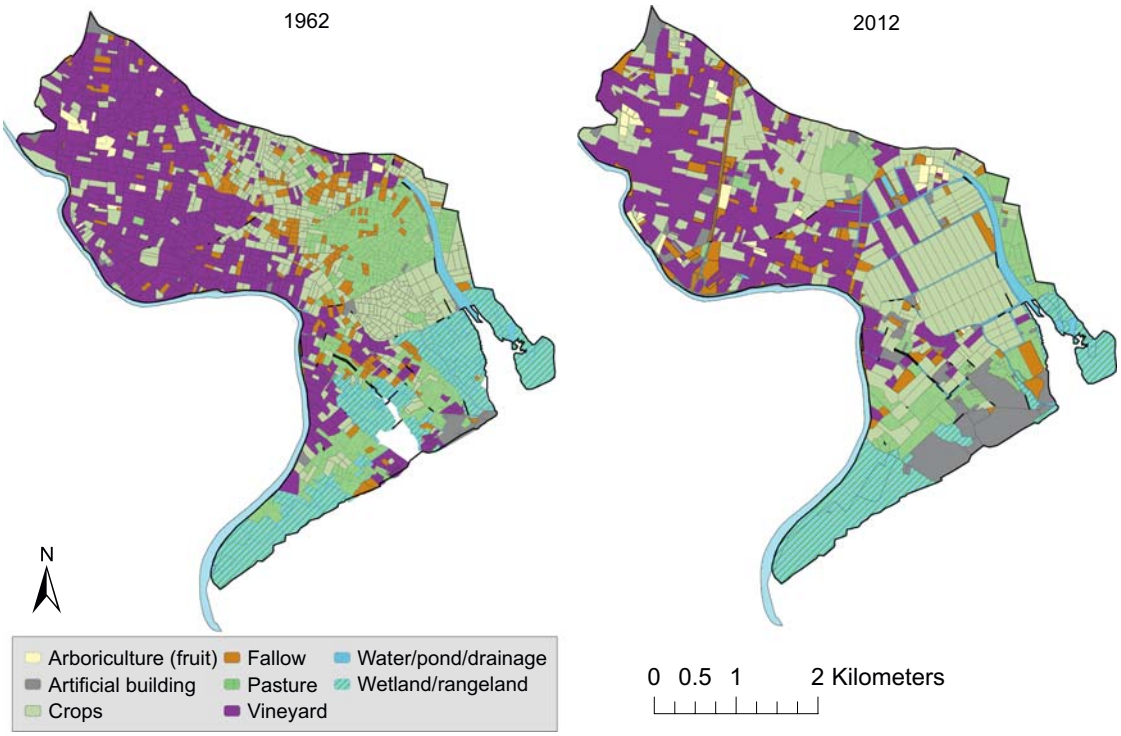

Fig. 3. Maps of land uses in the year 1962 and 2012.

Locally, geochemical analyses confirmed that the main ions in piezometer saturated zones were Na^+ and Cl^-, even if additional chemical species could contribute to ionic strength (Table 1).

At the landscape scale, seawater is the main source of Na^+ and Cl^-, but the analysis of the spatial structure of both $EC_{1/5}$ and EC_w (Fig. 2) shows that the spatial effect of the river on both soil and saturated zone salinity is greater than that of the sea. The river contains salts and is the most variable water source (standard deviation = 13.81 dS m^{-1}) (Table 1). The observed variability in the river water is linked to river discharges and seawater intrusions over time: depending on river discharge, seawater intrusion could be facilitated. Thus, decreased flow resulted in increased salt concentration (Isidora, 2011). Complementary observations (not shown) indicate that $EC_{1/5}$ values increased with increasing soil depth, then for higher proximity to saturated zone where salt accumulated as suggested by Greene et al. (2016).

Based on these observations, we assumed that underlying salt influxes were (i) from the sea to the river through seawater intrusion occurring during low flow periods, (ii) from the river to the saturated soil zone through river water infiltration at the embankments, and (iii) from the deep saturated zone to the root zone through waterlogging variations during the wet season and potential capillarity increases in the dry season. However, in order to determine the landscape salt budget, it is necessary to discuss potential salt outflows. For this, we focused on the ditch network, whose primary function is water and salt exportation as described by de Louw et al. (2011, 2013). The collected water sources were (i) water that percolates within the soil profile, (ii) water from the saturated zone, and (iii) excess runoff water that cannot infiltrate. Runoff water could be considered negligible in our context as field borders are often shaped to maximize within-field water infiltration (water harvesting technique). Origins and residence time of collected water in the inefficient network explain EC_w values associated with ditch network and network outlet: when collected, water in the percolation and saturated zones has similar conductivities when compared to that observed in the soil body, but the salts will concentrate due to evaporation. Higher mean and median values for the network outlet are linked to its geographical position, which is connected to the coastline and subjected to potential direct seawater contributions as reviewed by Daliakopoulos et al., 2016.

4.2. Conceptual model and landscape evolution

Previous findings and hypotheses allowed us to construct a preliminary version of the conceptual model proposed in Fig. 6 by combining main landscape constitutive elements: (i) the sea, the main source of salts, (ii) the river, the main source of fresh water and a source of saline water, (iii) the atmosphere, source and sink of fresh water, (iv) the land system, composed of three sub-systems (land use and cover, which modifies local water budget; soil, which is the main support for agricultural production and the reserve for plant roots uptakes; and the water table or saturated zone, which is the main plant available water reserve), and (v) humans, whose actions modify all constitutive elements. All of these elements interact through processes mentioned in the conceptual model (Fig. 6), for which we assumed that the system is in equilibrium. When applied to our study, the first order assumption was to consider that old conditions (pre-1962) allowed the reaching of the equilibrium state favorable for wine production by maintaining salinity at a sustainable level. Subsequently, in order to explain actual salinization, we used landscape evolution analysis to identify developments responsible for the system disequilibrium as proposed by Kingwell and John (2007) and Payen et al. (2016).

Among the changes cited by farmers is the evolution of landscape structure and the decrease in annual rainfall and river discharge. This disclosure by farmers demonstrated that for them the main issue in soil salinity management is the total available amount of fresh water for salt leaching from the soil root zone to the ditch network. Our aim was to conduct this time-series analysis for the period of 1960–2015 for each of the following conceptual model constitutive elements: atmosphere, river, and land system.

For atmosphere, the ET0 significantly increased over the 1960–2015 period. Time evolution for rainfall was less clear but nonetheless indicated a slight decrease with high interannual variability. Over time, the combination of these two trends for ET0 and rainfall has led to the

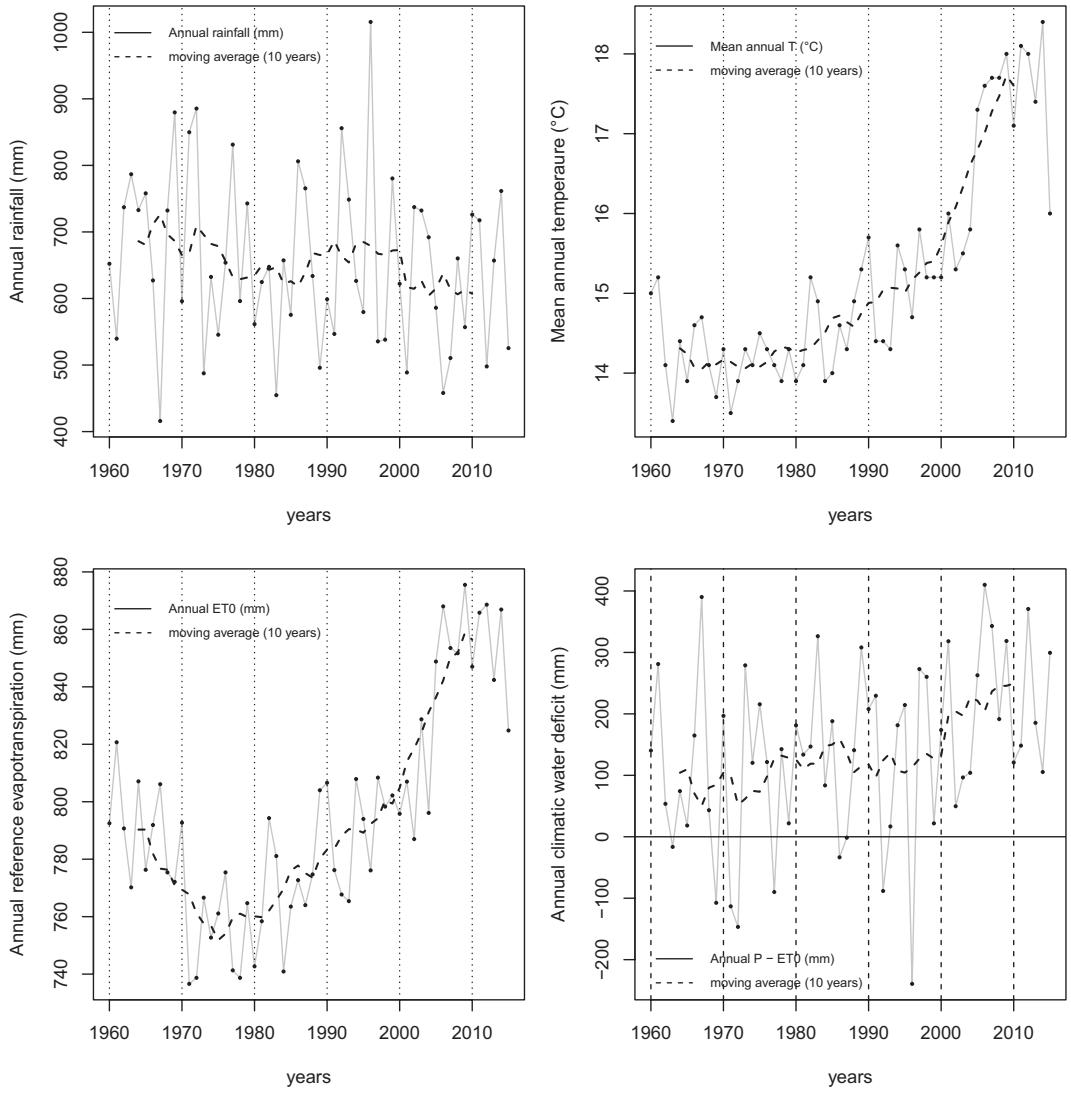

Fig. 4. The regional annual means of rainfall, temperature, and reference evapotranspiration (ET0) over the 1960–2015 period.

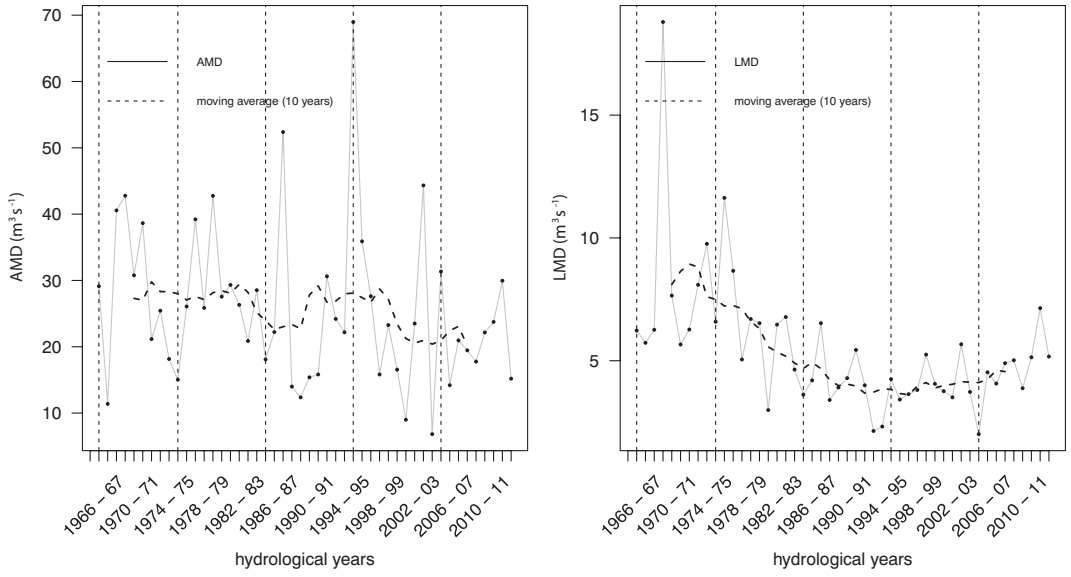

Fig. 5. The annual mean discharges (AMD) and the lowest monthly discharges (LMD) per year of the Orb River over the 1965–2015 periods at the Béziers-Tabarka station.

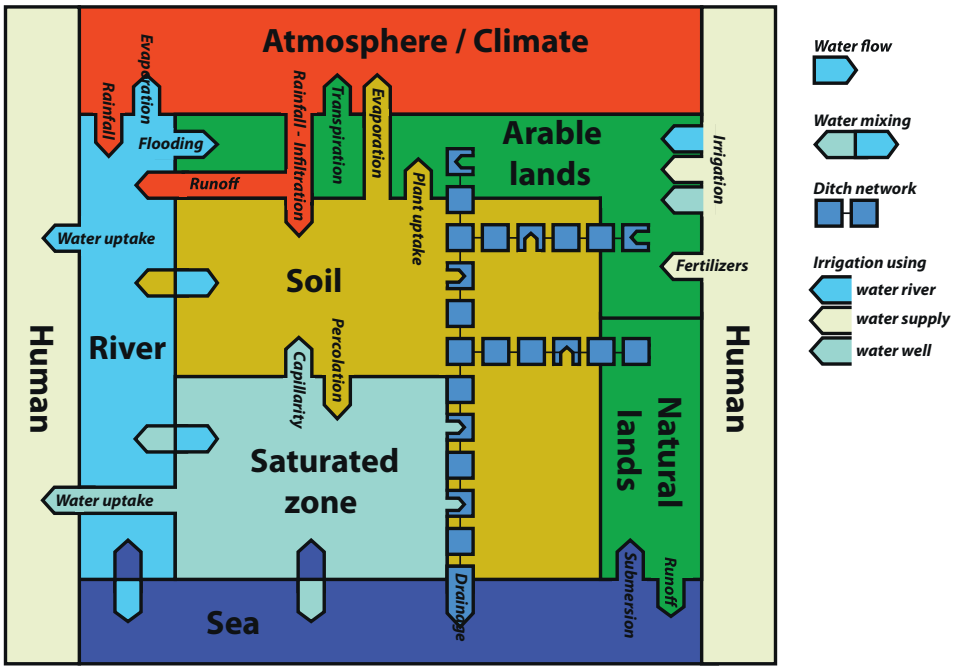

Fig. 6. Conceptual model of water fluxes in a coastal area affected by salinization.

multiplication of the climatic water deficit by a factor of 3 over the last 50 years (Fig. 4). When considering the seasonality of the Mediterranean climate, the consequences of such water deficit during the dry season include the following: (i) increased evaporation, leading to salt precipitation within the soil profile or on the soil surface, (ii) increased plant water uptake, leading to dryer conditions in the root zone, (iii) increased capillary forces acting in the soil body, favoring water and salt transfer in soil profiles from saturated to non-saturated zones (i.e., from the deeper soil horizon to the root zone) (Metternicht and Zinck, 2008), and (iv) decreased plant water uptake, as under SAS conditions in the root zone, plants are incapable of efficient water uptake (Rengasamy, 2010). Subsequently, the increased water stress for plants may lead to their mortality.

For rivers, analysis of AMD revealed no clear trend over time. The evolution of annual water flow in the river could not be interpreted in terms of salt pressure on the study area. However, despite interannual hydrological variability, LMD values have been low and stable since the mid-1980s. The stable LMD value is close to the French legal value of 2.5 $m^3 s^{-1}$. One realistic explanation of such a value is the regulation by water users of the discharges along the river over the past 30 years. Whatever the explanation might be, the consequence is increased seawater intrusion into the river.

For the land system, global landscape transition analysis demonstrates that land use and land dimensioning strongly evolved over the past 50 years. This landscape evolution was responsible for water table level evolution, as identified by Wu et al. (2014) as an important factor influencing soil salinization in alluvial plain. Fig. 7 illustrates the interactions between the ditch network and processes controlling water and salt availability in the root zone for different land system conditions. In this representation, the main processes are (i) evaporation and plant transpiration inducing decreased water content in the root zone, (ii) water infiltration from the soil surface to topsoil, (iii) capillary forces that create water and salt transfer from the saturated zone to topsoil horizons, (iv) percolation of water and dissolved salts (leaching) from the root zone to deeper soil horizons and the saturated zone, (v) water exchange and mixing in the saturated zone or, more generally, groundwater in the alluvial compartment and the associated river, and (vi) drainage of the saturated zone by the ditch network. For the first set of land system conditions, corresponding to a theoretical condition without the ditch network, the maximum water table level rises to near the soil surface (H0). Here, under saline groundwater conditions the consequence is salinization of the whole soil profile. The second set of land system conditions corresponds to the high density of ditch structures as observed prior to 1962. Here, ditch density leads to a maximum reduction of the water table to the maximum H1 level. The third condition indicates the evolution of drainage density that occurred between the 1960s and 2012, the effect of which was to induce less water table reduction when compared to the previous set of conditions, with a reduction in the maximum water table level at the H2 elevation. The last condition is equal to the third but integrates the maintenance default of the drainage network responsible for ditch filling and decreasing the overall network efficiency for water table control, with a maximum H3 level for the saturated zone. For this last set of land system conditions, the increase of the H3 level leads to waterlogging and salt accumulation in the root zone.

Another dimension of the land system is the evolution of land use type allocation in space and time (Fig. 3). The overall transition was to a net decrease in total area of both vineyards and pastures, whereas the total area for crops and building increased. With time, most of the vineyard located close to the coastline was replaced by residential buildings. Historically, this substitution might be due to lower productivity of wine in the area as a result of severe damage by salinization, then a distribution of cultivated plants due to the tolerance to soil salinity as observed by Bas et al. (2017) in coastal cropping systems. It also might be due to economic pressure induced by increasing numbers of tourism activities over the past 50 years. The tourism dimension was responsible for the increased number of residential buildings in the coastal area and reduced total area of wetland and rangeland, which collected saline water from fields, creating a buffer area between the coastline and arable lands. Mechanization was as a major driver for landscape change: mechanization has triggered increasing size of field units and the associated transition from horses to engines has rendered pastures useless.

When viewed together, the abovementioned developments have been responsible for the disruption of the system equilibrium, favoring overall salt accumulation in the soil root zone. The main driving factor of water and soil salinization in this area was mainly influxes of seawater through the river, which intruded into the saturated zone and entered the soil through the seasonal variation in waterlogging and capillarity.

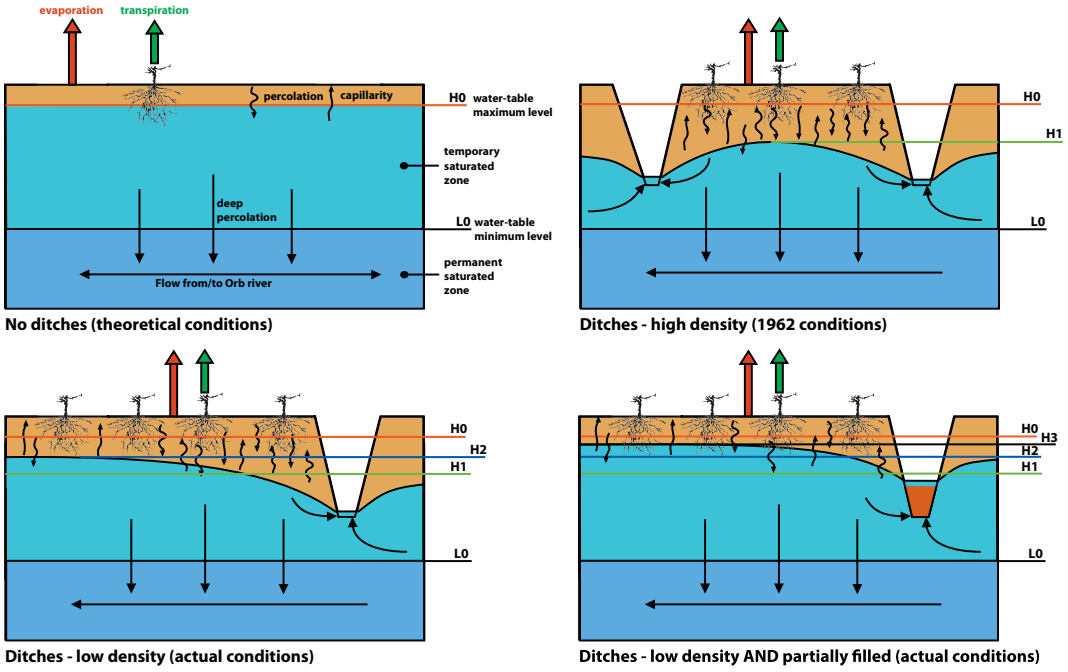

Fig. 7. Interactions between the ditch network and processes controlling water and salt availability in the root zone for different land system conditions.

Natural and anthropogenic evolution such as land use, rainfall, temperature, river discharge, and agricultural practices, which are noticeable at the landscape scale, impacted the salinization process. Mechanization practices have led to the reshaping of agricultural fields from 1960 to 2012 and caused the modification of the drainage channel network and reduced efficiency of drainage function to drain saline water from the field. Declining rainfall and increasing temperatures over the last decade have directly impacted local water balance in the study area and probably changed the intensity of capillary saline water fluxes. The hydrological regime of the river played a central role, since the flood events and pumping are sources of field submersion with fresh water, and low flow magnitudes defined seawater intrusion into the river and associated alluvial groundwater. Thus, the solution may lie in overall river catchment water policy and local adaptation involving land use repartitioning, soil management, submersion and drainage practices.

5. Conclusion

Investigations of both soil and water electrical conductivity of agricultural lands in Sérignan allowed us to characterize spatial structures of soil and water salinity affecting vine production and to identify the river as a preponderant factor in land salinization. We subsequently proposed a conceptual model for water fluxes in the coastal agricultural area. Main landscape elements (sea, river, atmosphere, land use and cover, soil, water table, and humans) and processes constitute this simple model. This model, when coupled with time analyses of climate, river, and land systems since 1960, helped us to understand the main evolutionary processes responsible for the disruption of system equilibrium, favoring overall salt accumulation in the soil root zone: (i) a decrease of freshwater influx due to river discharge evolution, (ii) an increase of freshwater outflow due to climate evolution, (iii) an increase in saline water influx due to seawater intrusions into the river, and (iv) a decrease in saline water outflow due to ditch network evolution.

Acknowledgment

The authors acknowledge farmers' cooperative in Sérignan France for all supports and cooperation during data collection. The acknowledgment also goes to ALFABET funding project of Erasmus Mundus that supporting first author to pursue PhD. We are grateful for the valuable comments and suggestions provided by three anonymous reviewers.

Appendix A. Supplementary data

Supplementary data to this article can be found online at https://doi.org/10.1016/j.scitotenv.2017.12.083.

References

Barriere, J., Malacarne, J., Mazier, J., 1973. Carte des sols au 1/5000e – sérignan 10_24_m–la grande maïre 10_24_n 1,2,3,4 – les orpellières 9_24_b 1,2,3. Caractéristques principales et classement pédogénétique. B. Rh. L. - SAGEM – SOLEM – 685 Route d'Arles 30001, Nîmes, France.

Bas, Niñerola V., Navarro-Pedreño, J., Lucas, I.G., Pastor, I.M., Vidal, M.M.J., 2017. Geostatistical assessment of soil salinity and cropping systems used as soil phytoremediation strategy. Remediat. Polluted Soil Part 1 (174):53–58. https://doi.org/10.1016/j.gexplo.2016.06.008.

Bless, A.E.S., Colin, F., Crabit, A., Devaux, N., Philipon, O., Follain, S., 2017. Sols salins et sodiques. Cas de sols de Sérignan (Hérault, France). Note technique de Montpellier SupAgro (10 pp.).

Brechin, S.R., Wilshusen, P.R., Fortwangler, C.L., West, P.C., 2002. Beyond the square wheel: toward a more comprehensive understanding of biodiversity conservation as social and political process. Soc. Nat. Resour. 15 (1), 41–65.

Cave cooperative de viticulteurs de Sérignan, 2016. Analyses de terre des viticulteurs de Sérignan. Documents internes.

Claessens, L., Schoorl, J.M., Verburg, P.H., Geraedts, L., Veldkamp, A., 2009. Modelling interactions and feedback mechanisms between land use change and landscape processes. Agric. Ecosyst. Environ. 129, 157–170.

Coletti, J.Z., Vogwill, R., Hipsey, M.R., 2017. Water management can reinforce plant competition in salt-affected semi-arid wetlands. J. Hydrol. 552:121–140. https://doi.org/10.1016/j.jhydrol.2017.05.002.

Custodio, E., 2002. Coastal Aquifers as Important Natural Hydrogeological Structures. Groundwater and Human Development (ISBN 978-544-063-9).

Daliakopoulos, I.N., Tsanis, I.K., Koutroulis, A., Kourgialas, N.N., Varouchakis, A.E., Karatzas, G.P., Ritsema, C.J., 2016. The threat of soil salinity: a European scale review. Sci. Total Environ. 573:727–739. https://doi.org/10.1016/j.scitotenv.2016.08.177.

de Louw, P.G.B., Eeman, S., Siemon, B., Voortman, B.R., Gunnink, J., van Baaren, E.S., Essink, O.G.H.P., 2011. Shallow rainwater lenses in deltaic areas with saline seepage. Hydrol. Earth Syst. Sci. 15, 3659–3678.

de Louw, P.G.B., Eeman, S., Essink, G.H.P., Vermue, E., Post, V.E.A., 2013. Rainwater lens dynamics and mixing between infiltrating rainwater and upward saline groundwater seepage beneath a tile-drained agricultural field. J. Hydrol. 501:133–145. https://doi.org/10.1016/j.jhydrol.2013.07.026.

EEA, 2000. Down to earth: soil degradation and sustainable development in Europe. A challenge for the 21th century. United Nation Convention Fourth Conference of the Parties Bonn, 19 December 2000.

Feinerman, E., Yaron, D., Bielorai, H., 1982. Linear crop response functions to soil salinity with a threshold salinity level. Water Resour. Res. 18, 101–106.
Gkiougkis, I., Kallioras, A., Pliakas, F., Pechtelidis, A., Diamantis, V., Diamantis, I., Ziogas, A., Dafnis, I., 2015. Assessment of soil salinization at the eastern Nestos River Delta, NE Greece. Catena 128, 238–251.
Greene, R., Timms, W., Rengasamy, P., Arshad, M., Cresswell, R., 2016. Soil and aquifer salinization: toward an integrated approach for salinity management in of groundwater. Integrated Groundwater Management https://doi.org/10.1007/978-3-319-23576-9_15.
Harris, I., Jones, P.D., Osborn, T.J., Lister, D.H., 2014. Updated high-resolution grids of monthly climatic observations – the CRU TS3.10 dataset. Int. J. Climatol. 34: 623–642. https://doi.org/10.1002/joc.3711.
IPCC, 2014. In: Core Writing Team, Pachauri, R.K., Meyer, L.A. (Eds.), Climate Change 2014: Synthesis Report. Contribution of Working Groups I, II and III to the Fifth Assessment Report of the Intergovernmental Panel on Climate Change. IPCC, Geneva, Switzerland (151 pp.).
Isidora, D., 2011. River salt loads as influenced by Irrigation development in the Bardenas Irrigation Scheme (Spain). Proceeding of Global Forum in Salinization.
Jahn, R., Blume, H.P., Asio, V.B., Spaargaren, O., Schad, P., 2006. Guildlines for Soil Description. FAO.
JRC, 2012. The State of Soil in Europe. JRC Reference Reports. European Environment Agency. European Union.
Kingwell, R., John, M., 2007. The influence of farm landscape shape on the impact and management of dryland salinity. Agric. Water Manag. 89, 29–38.
Li, J., Pu, L., Zhu, M., Zhang, R., 2012. The present situation and hot issues in the salt-affected soil research. Acta Geograph. Sin. 67 (1233–1245), 2012.
Maas, E.V., Hoffman, G.J., 1977. Crop salt tolerance-current assessment. J. Irrig. Drain. Div. 103, 115–134.
Margoluis, R., Stem, C., Salafsky, N., Brown, M., 2009. Using conceptual models as a planning and evaluation tool in conservation. Eval. Program Plann. 32 (2), 138–147.
Martinez-Beltran, J., Manzur, C.L., 2005. Overview of salinity problems in the world and FAO strategies to address the problem. Proceedings of the International Salinity Forum, Riverside, California, April 2005, pp. 311–313.
Metternicht, G., Zinck, A., 2008. Remote Sensing of Soil Salinization: Impact on Land Management. CRC Press.
Michot, D., Walter, C., Adam, I., Guéro, Y., 2013. Digital assessment of soil-salinity dynamics after a major flood in the Niger River valley. Geoderma 207–208, 193–204.
Hannah, L., Midgley, G.F., Lovejoy, T., Bond, W.J., Bush, M., Lovelett, J.C., et al., 2002. Conservation of biodiversity in a changing climate. Conserv. Biol. 16 (1), 264–268.
Payen, S., Basset-Mens, C., Núñez, M., Follain, S., Grünberger, O., Marlet, S., Perret, S., Roux, P., 2016. Salinisation impacts in life cycle assessment: a review of challenges and options towards their consistent integration. Int. J. Life Cycle Assess. 21, 577–594.
Potter, I.C., Chuwen, B.M., Hoeksema, S.D., Elliot, M., 2010. The concept of an estuary: a definition that incorporates systems which can become closed to the ocean and hypersaline. Estuar. Coast. Shelf Sci. 87:497–500. https://doi.org/10.1016/j.ecss.2010.01.021.
Rengasamy, P., 2006. World salinization with emphasis on Australia. J. Exp. Bot. 57 (5): 1017–1023. https://doi.org/10.1093/jxb/erj108 (Plants and Salinity Special Issue).
Rengasamy, P., 2010. Soil processes affecting crop production in salt-affected soils. Funct. Plant Biol. 37, 613–620.
Rhoades, J., 1997. Salinity: electrical conductivity and total dissolved solids. Methods Soil Anal. Part 3-Chemical Methods, pp. 417–435.
Rhoades, J., Chanduvi, F., Lesch, S., 1999. Soil Salinity Assessment: Methods and Interpretation of Electrical Conductivity Measurements. Food & Agriculture Org. (FAO).
Richard, L.A., 1954. Diagnosis and Improvement of Saline and Alkaline Soils. Agricultural Handbook No.60. US Department of Agriculture https://www.ars.usda.gov/pacific-west-area/riverside-ca/us-salinity-laboratory/docs/handbook-no-60/ (accessed 26.27.2017).
Richards, L.A., 1974. Diagnostico y rehabilitacion de suelos salinos y alkalios. Limusa, Mexico.
Rounsevell, M.D.A., Ewert, F., Reginster, I., Leemans, R., Carter, T.R., 2005. Future scenarios of European agricultural land use: II. Projecting changes in cropland and grassland. Agric. Ecosyst. Environ. 107, 117–135.
Salome, C., Coll, P., Lardo, E., Villenave, C., Blanchart, E., Hinsinger, P., Marsden, C., Le Cadre, E., 2014. Relevance of use-invariant soil properties to assess soil quality of vulnerable ecosystem: the case of Mediterranean vineyards. Ecol. Indic. 43:83–93. https://doi.org/10.1016/j.ecolind.2014.02.016.
Shrestha, R.P., 2006. Relating soil electrical conductivity to remote sensing and other soil properties for assessing soil salinity in northeast Thailand. Land Degrad. Dev. 17, 677–689.
Szabolcs, D.L., 1985. Salt affected soils as a world problem. The Reclamation of Salt-Affected Soils. Proceedings of the International Symposium Jinan, China. Beijing Agricultural University, Beijing, pp. 30–47.
Szabolcs, I., 1992. Salinization of soil and water and its relation to desertification. Desertification Bulletin. vol. 21, pp. 27–32.
Thornthwaite, C.W., 1948. An approach toward a rational classification of climate. Geogr. Rev. 38:55–94. https://doi.org/10.2307/210739.
Tóth, G., Montanarella, L., Rusco, E., 2008. Threats to Soil Quality in Europe. JRC Scientific and Technical Report. EUR 23438-Scientific and Technical Research Series. Off. Publi. Eur. Communities Luxemb. pp. 61–74.
Verburg, P.H., Soepboer, W., Veldkamp, A., Limpiada, R., Espaldon, V., 2002. Modelling the spatial dynamics of regional land use: the CLUE-S model. Environ. Manag. 30, 391–405.
Whitfield, A., Elliot, M., 2011. Ecosystem and biotic classifications of estuaries and coasts. Treatise on Estuarine and Coastal Science. Academic Press, Waltham, pp. 99–124.
WRB, 2015. World Reference Base for Soil Resource 2014, International Soil Classification System for Naming Soils and Creating Legends for Soil Maps. Food and Agriculture Organization of The United Nations, Rome, Italy.
Wu, J., Li, P., Qian, H., Fan, Y., 2014. Assessment of soil salinization based on a low-cost method and its influencing factors in a semi-arid agricultural area, northwest China. Environ. Earth Sci. 71:3465–3475. https://doi.org/10.1007/s12665-013-2736-x.